Decision Support Systems 177 (2024) 114078

Contents lists available at ScienceDirect

Decision Support Systems

journal homepage: www.elsevier.com/locate/dss

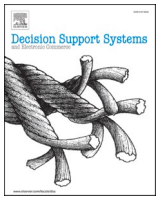

A functional Hidden Markov Model to incorporate dynamics into Bayesian optimal stopping problems: Helping physicians manage traumatic brain injuries

Gleb Zavadskiy *, Daniel Zantedeschi, Wolfgang Jank

School of Information Systems and Management, Muma College of Business, University of South Florida, USA

ARTICLE INFO

Keywords:
Decision support systems
Functional data analysis
Hidden Markov Models
Markov Chain Monte Carlo
Bayesian optimal stopping
Traumatic brain injuries
Healthcare

ABSTRACT

This paper describes a decision support system for neurosurgeons to determine the release schedule for polytrauma patients with concurrent traumatic brain injuries (TBIs). We present a novel functional Hidden Markov Model (fHMM) designed to mitigate the computational burden caused by ever-growing historical data. Our fHMM is nested into a Bayesian optimal stopping problem, effectively representing emergency physicians' crucial decisions during the discharge process. Our model is unique in its ability to adapt to different physician decision-making styles while continuously monitoring patient progress. We validate our approach using simulated and real data from a major hospital in Tampa Bay. The analysis reveals that dynamic prognostic measures can help balance the competing needs of rapid patient release and neurologic stability. Additionally, our results show variability in physicians' expectations regarding neurological recovery. Counterfactual analyses suggest that implementing this decision model could potentially save up to $27,500 per TBI patient under certain conditions.

1. Introduction

In healthcare management, doctors must closely monitor a patient's condition to decide on the form of care dependent on the expected disease course [1–4]. Once a doctor determines the type and start of the clinical intervention plan, irreversible damage might occur if the patient's condition is not stable enough to sustain the procedure [4]. In that sense, a doctor needs to make an optimal decision, balancing gathering information with the start of the intervention. This paper develops a decision support system for neurosurgeons and healthcare professionals to make optimal stopping decisions sequentially [4].

Optimal stopping algorithms have been extensively studied in decision support systems and healthcare [5–12]. This paper introduces a functional Hidden Markov Model (fHMM) that incorporates the entire history of observations into decision-making [13]. Using a functional framework overcomes the computational challenges associated with the continuously growing stream of information in sequential decision-making, where an intervention decision on a specific day depends on a doctor's observations of a patient from the current day and observations and decisions from previous days [5]. Using functional data concepts, our approach preserves the Markovian structure and reduces the problem's dimensionality [13]. In addition, it incorporates the dynamics of prognostic scores [14–16], allowing physicians to assess the speed and the change in speed of a patient's development.

Our approach also allows for personalized decision-making, which is essential as patients within the same illness category often exhibit very heterogeneous symptoms and require individualized treatment plans [17]. Separating heterogeneity from forward-looking behavior poses a challenge in decision models [17]. We overcome this by setting a constant but heterogeneous discount rate across physicians, which aligns with short-term forward-looking behavior and healthcare evaluation practices [18].

We apply the fHMM framework to Bayesian optimal stopping problems in healthcare to help surgeons decide on the optimal release time of patients with traumatic brain injuries (TBIs) within the first 24 to 48 h of polytrauma. Our findings suggest prioritizing brain recovery over addressing other trauma for patients with high intracranial pressure (ICP) and head computed tomography (CT) scores [19]. Additionally, patients with low Glasgow Coma Scale (GCS) and high ICP scores are likely to have longer stays in the neurosurgical unit. Furthermore, our results indicate that doctors should prioritize the current CT score and the previous day's release probability when considering patient release. We also highlight variations in physicians' decision-making approaches, with some relying solely on past dynamics of prognostic scores rather

* Corresponding author at: School of Information Systems and Management, Muma College of Business, 4202 E. Fowler Avenue, Tampa, FL 33620, USA.
E-mail addresses: zavadskiy@usf.edu (G. Zavadskiy), danielz@usf.edu (D. Zantedeschi), wjank@usf.edu (W. Jank).

https://doi.org/10.1016/j.dss.2023.114078
Received 9 January 2023; Received in revised form 29 August 2023; Accepted 4 September 2023
Available online 7 September 2023

than adopting a forward-looking perspective. Finally, we quantify the average cost reduction for different traumatic brain injury severity levels.

2. Related literature

Hidden Markov Models (HMMs) have found a wide range of applications in different research areas [5,6,8,20–22]. The core idea of HMMs is that there are two sequences: latent states and observables. At each point in time, an agent wants to infer the latent state of the system given the observed information. Examples of using HMM in healthcare information technology include Ayabakan, Bardhan and Zheng [23] and Yan and Tan [24].

In contrast to these prior applications, we nest the HMM structure within an optimal stopping framework, known as a partially observable Markov Decision Process (POMDP) [25]. The POMDP framework makes the modeled world closer to reality, where an agent can perform an action based on partial observations, i.e., when the true state of the system is hidden (but the agent observes some information about the system). One of the earliest applications of HMM to search problems is discussed in Hartman and van Hee [26]. Since then, many alternate applications of Markov Decision Process (MDP) have been applied to optimal stopping in decision support systems, e.g., [5–8,27]. However, none of these applications incorporate the entire information history via the idea of functional modeling.

Existing approaches to solving POMDPs in healthcare see [14,28–32] are not suited to our problem. First, most extant approaches consider a stationary transition matrix for the evolution of the states. Our paper allows the probabilities to differ given some features, e.g., time, the functional form of observations, etc. Second, extant approaches typically assume the Markov property, i.e., the subsequent period distribution of states depending only on the present state and not on past states. And third, current observations relate to the previous observations through state transitions only. We instead include all the past observations through their functional representation inferred at each point in time. Finally, the most important distinguishing feature is that we cut the feedback from states. In the full Bayesian model, the information from states flows back to influence posterior distributions of imputed values in the first phase [33]. To preserve computational tractability, we "cut this feedback" by reverting the dependency between observations and states (see Section 3).

Our approach differs from the one implied by variable-length Markov chains [34] in that the latter will grow with each additional period. In contrast, in our approach, each additional period merely changes the functional representation but does not add to the dimensionality of the model. Another interesting modification of the traditional HMM is fractional HMM [35]. This algorithm uses the special structure of HMM with distributed state representation. However, this type of model uses only current observation to decide on the hidden state, while our model incorporates the past dynamics through functional representation of observations. Additionally, given the current observation, the fractional HMM keeps track of all underlying Markov models and switches between them. The latter can be computationally hard for large datasets.

POMDPs aim to maximize the reward given states and actions over time. In contrast, in our paper, we find the optimal stopping time that maximizes the reward function given states and actions over time. Solving the optimal stopping problem for a hidden Markov chain is also known as a sequential tracking problem e.g., [7,27,36,37], using Bayesian updates given the values of observed variables; however, while extant approaches use the Bayesian updates over the discrete observations, we use a functional form of observations.

Other examples of applying the Bayesian framework for sequential decision-making problems are Chick, Forster and Pertile [38], Pertile, Forster and La Torre [39], and Dai, Yu, Low and Jaillet [40]. The first two groups apply the Bayesian paradigm to the sequential and adaptive trial design problem. Specifically, Pertile, Forster and La Torre [39] develop a Bayesian sequential model and apply it to a case of randomized clinical trials. Chick, Forster and Pertile [38] extend the previous paper and propose a Bayesian-based, fully sequential decision framework to choose the optimal policy for healthcare technology adoption. In their paper, Dai, Yu, Low and Jaillet [40] move further and combine Gaussian process-upper confidence bound (i.e., Bayesian optimization) with Bayesian optimal stopping "in a natural way to derive a principled mechanism for optimally stopping hyperparameter evaluations during BO" [40], p. 8.

We apply our method to the problem of releasing patients with TBI for further non-cranial surgical interventions and extend the results by Zavadskiy, Zantedeschi and Jank [41]. To our knowledge, medical field researchers only use basic HMM to track patients with traumatic brain injuries, e.g., Schaefer, Bailey, Shechter and Roberts [42]. Many authors e.g., [43,44–47] found a Markovian structure to be suitable for predicting outcomes for clinical patients with traumas associated with highly uncertain health conditions, such as brain injuries. For example, Asgari, Adams, Kasprowicz, Czosnyka, Smielewski and Ercole [44] and Myers, Lazaridis, Jermaine, Robertson and Rusin [46] have made successful attempts to predict a patient's crisis after TBI using different neurological scores as predictors. From the methodological point of view, the last two sets of authors mentioned above applied HMMs for their desirable properties when dealing with patients transitioning between partially observable health states. Moreover, these models allow accounting for both types of heterogeneous behavior using a recursive structure and time dependency of readings through transition probabilities.

However, while prior approaches assume that an analyst simply wishes to infer how a system evolves without taking action based on the system's status, a neurosurgeon must decide daily (similar to POMDPs). In the medical field, POMDPs have been found useful for various types of diseases [14,15,28–32,48–50]. In contrast to extant approaches, we use the patient's individual history of readings to predict their readiness to undergo a non-cranial surgery.

3. Bayesian optimal stopping and functional HMM

In this section, we start by discussing the general structure of HMMs. Then, we develop the functional HMM, which allows us to incorporate the entire history of observations. And lastly, we create an optimal stopping framework for the fHMM.

3.1. HMM

A Markov process describes a sequence of possible events (or states) with a certain probability of moving from one state to another. A Hidden Markov Model is a statistical model in which the system to be modeled is assumed to follow a Markov process with unobservable (or hidden) states and observations conditioned on those states.

Let S be a finite set of states and Y be a set of sequences of observations y, such as $y = y_1,\ldots,y_t$. For a traditional homogeneous HMM, at each time point $t \in T$, we can write the probability of transitioning from state j to state i given the previous state as $P(S_t = j|S_{t-1} = i) = \gamma_{ij}$ and the probability of observing the data given the current state as $P(y_t|S_t = i)$.

Following McCallum et al. [51], we replace the transition probability function and the observation probability function with $P(S_t = j|S_{t-1} = i, y_t)$. This allows us to overcome two problems with traditional HMMs. First, the richer representation of observations increases the accuracy of prediction. Second, given the observation sequence, we want to predict a state sequence in many tasks. This replacement cuts the information feedback from states to observations described by Plummer [33]. Further, we add functional data analysis to distinguish our model from the one proposed by McCallum, Freitag and Pereira [51].

3.2. Functional HMM

The Markov property of an HMM assumes that the present state carries all information needed to infer the system's future state. In other words, it assumes that the past does not influence the future. In this paper, we want to use the entire history of observations because it frequently plays an essential role in defining a latent state. For instance, a good (bad) dynamic of patient's scores may positively (negatively) affect a doctor's judgment about the current state of a patient given the current readings. Extensions of the first-order Markov property, such as the second-order or third-order Markov property, incorporate information about one immediate past state, two immediate past states, etc. However, with a continuously growing number of time periods, the order of the Markov property would grow infinitely. Thus, incorporating the entire history of observations is computationally challenging. To bypass this, we represent histories as functions and use their properties to define a system's latent state.

In the functional representation, $P(S_t = j|S_{t-1} = i, y_t)$, can be expanded to $P(S_t = j|S_{t-1} = i, f(y_t), E_t(f(y)))$. Fig. 1 illustrates the difference between a traditional HMM, the extended model suggested by McCallum, Freitag and Pereira [51] and our fHMM. Here, S_1, S_2, and S_3 are latent states, Y_1, Y_2, and Y_3 are observations, $f(Y_t)$ is a function of observations at time t, and $E(f(Y))$ is the expected value of observation at the next step.

To operationalize our fHMM, we employ ideas from *functional shape analysis* (FSA) [52], using three steps. We first smooth the observed histories to eliminate noise from the raw data. Next, we apply functional principal component analysis to decompose the smooth histories and extract key shapes, and then we use the most important shapes to predict the latent state.

In the first step, we smooth the observed histories using a penalized smoothing spline: given a set of knots $\tau_1 \ldots \tau_L$, a penalized smoothing spline is given by a polynomial of order p $f(t) = \beta_0 + \beta_1 t + \ldots + \beta_p t^p + \sum_{l=1}^{L} \beta_{pl}(t - \tau_l)_+^p$ which minimizes the penalized squared error $PENSS_{\lambda,m} = \int [y(t) - f(t)]^2 dt + \lambda \int [D^m f(t)]^2 dt$, where $y(t)$ denotes the observed data at time t and $D^m f$ denotes the *mth* derivative of the function f.

In the second step, we obtain the functional principal components of the smooth histories in a way similar to the ordinary principal component analysis. Let the principal component scores (PCS) be defined as the inner product of smooth histories $y_i(t) = [y_{i1}, \ldots, y_{ip}]$ (evaluated over a fine grid) and the corresponding principal components $PC_j = [e_{j1}, \ldots, e_{jp}]$, i.e., $PCS_{ij} = y_{i1}e_{j1} + .. + y_{ip}e_{jp}$. Each PCS now characterizes one component of the shape of the smooth history $y_i(t)$ [52].

Finally, in the third step, we determine the most important shape components by selecting only those principal components that account for the most variation in the data. Using this decomposition, $P(S_t = j|S_{t-1} = i, f(y_t), E_t(f(y)))$ becomes

$$P\Bigg(S_t = j|S_{t-1} = i, \mu(t) + \sum_{m=1}^{M} PCS_m(t), E(\mu(t+1)) + \sum_{m=1}^{M} E\Big(PCS_m(t+1)\Big)\Bigg) \quad (1)$$

where $\mu(t)$ is a mean trend and $PCS_m(t)$ is the mth principal component score.

We incorporate the principal component scores into the Bayesian framework through the joint probability $P(f(y_t), E_t(f(y)))$. The main strength of the Bayesian framework is conditioning on information provided by data. We obtain the posterior distributions for parameters as a combination of prior distributions for the parameters ("initial" beliefs) and the likelihood function ("evidence" provided by data). It allows us to characterize uncertainty given the data and deal with scalable problems or problems where sample sizes are an issue.

3.3. Bayesian optimal stopping

An HMM only describes the transition probabilities between latent states given observations but does not tell a decision-maker when to stop making new observations. To that end, we need to add a stopping rule to the HMM balancing the costs and rewards for such a decision e.g., [36,37].

The general idea is that a controller chooses a range of policies from the finite set of strategies A and attempts to infer the unobserved state S given the observable information y. At each time point, the objective of a controller is to track a state of a system, given the observed information about it. The controller's overall strategy consists of a double sequence of (t_k, a_k), where $a_k \in A$ represents the sequence of policies and $0 \triangleq t_0 < t_1 < \ldots \leq T$ is a time of policy changes. Consequently, the overall objective is to maximize the total present value of all tracking benefits and costs associated with the applied strategy. In other words, let $V_\pi^* = \max_\pi V_\pi$ be the maximum present value of all benefits $R(S_t, a_t)$ and costs $C(S_t, a_t)$ associated with the optimal strategy π. Thus, we can write $V_\pi^* = \max_\pi V_\pi = \max_\pi (R_\pi(S_t, a_t) - C_\pi(S_t, a_t))$.

4. Parameter estimation via Markov Chain Monte Carlo

This section describes the parameter estimation process for our fHMM using Bayesian optimal stopping. We estimate all parameters on a training set using Markov Chain Monte Carlo (MCMC) [53,54]. The idea behind MCMC is to define a Markov chain of the sampling process that converges to the average of the true distribution of a parameter of interest. The main strength of MCMC is that it allows us to sample from the posterior distributions of the unknowns without the need of a closed-form solution [55,56].

We can write the maximum of the reward function as.

$$\max_\pi \Bigg(R_\pi(S_t, a_t)) = R_0 + \max_a \sum_{n=1}^{\infty} P(S_{t+n} = j|S_t = i, f(y_{t+n}), E_{t+n}(f(y)))^* R(S_{t+n}, a_{t+n}) \quad (2)$$

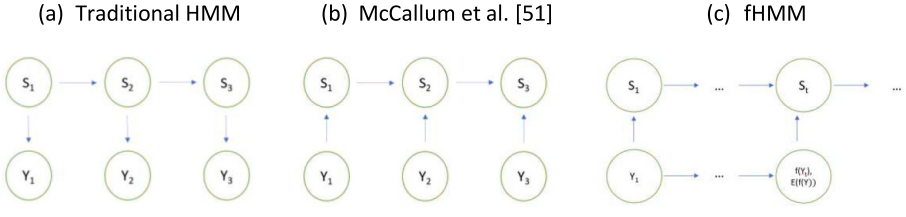

Fig. 1. Comparison of dependency graphs.

and similarly, the maximum of "minus" cost function (or its minimum) as.

$$\min_{\pi}\Bigg(C_{\pi}(S_t,a_t)) = C_0 + \min_{a}\sum_{n=1}^{\infty} P(S_{t+n}=j|S_t = i,f(y_{t+n}),E_{t+n}(f(y))\,)^{*}C(S_{t+n},a_{t+n}). \tag{3}$$

The probability observing state j at time point $t+n$ given the dynamics of observations at this time point and the expected one period ahead observation is simply a product of one-step transition probabilities, i.e.,

$$P(S_{t+n}=j|S_t = i,f(y_{t+n}),E_{t+n}(f(y))\,) = \prod_{m=1}^{n} P(S_{t+m}=j|S_{t+m-1} = i,f(y_{t+m}),E_{t+m}(f(y))\,). \tag{4}$$

The transition probabilities can be rewritten using a Bayes rule as.

$$P(S_{t+1}=j|S_t = i,f(y_{t+1}),E_{t+1}(f(y))\,) = \frac{P(S_{t+1}=j)^{*}P(S_t = i,f(y_{t+1}),E_{t+1}(f(y))\,|S_{t+1}=j)}{P(S_t = i,f(y_{t+1}),E_{t+1}(f(y))\,)}. \tag{5}$$

The denominator can be written as.

$$P(S_t = i,f(y_{t+1}),E_{t+1}(f(y))\,) = P(S_t = i)^{*}P(f(y_{t+1}),E_{t+1}(f(y))\,|S_t = i). \tag{6}$$

To estimate each parameter in the model, we should sample from the posterior joint distribution $P(S_t = i,f(y_{t+1}),E_{t+1}(f(y))\,|S_{t+1}=j)$. This is analytically complicated because it involves solving multidimensional integrals. Instead, rather than sampling from the joint distribution, MCMC allows us to sample from the following posterior distributions: $P(S_t = i\,|\,f(y_{t+1}),E_{t+1}(f(y))\,,S_{t+1}=j)$, $P(f(y_{t+1})\,|\,S_t = i,E_{t+1}(f(y))\,,S_{t+1}=j)$, and $P(E_{t+1}(f(y))\,|\,S_t = i,f(y_{t+1}),S_{t+1}=j)$. This allows us to treat only one parameter as a random variable and sample from its posterior distribution, keeping all other variables constant.

The following pseudocode illustrates the general learning sequence of our method. We iterate between steps two and five until convergence. Given the data, we declare convergence when maximizing the likelihood of the predicted states and observations' sequences. We want to point out that these steps can be readily converted into Stan code. Steps two through four pertain to Bayesian learning, where we update the probability for each latent state via Bayes theorem. Step five is the optimization part of the algorithm. Each time we return to step two to sample another decision, we recompute the probability of each decision again and again. Finally, we choose the one that is the most likely given our data. In other words:

1. Start iteration 0 with some arbitrary probability for each latent state, e.g., equal probabilities for all.
2. At iteration j, given the current function of observations, predict a future observation.
3. At the same iteration j, given the current function of observations, the predicted future observation, and the previous state, predict probabilities for each state in the current step.
4. Given obtained probabilities for each state at iteration j, calculate the expected reward for each action and choose the one maximizing rewards.
5. Return to step two.

5. Application to scheduling traumatic brain injuries

We now return to our application of managing traumatic brain injuries. In this section, we describe our data and explain how to apply our model to managing TBIs. In Section 6, we perform a simulation study based on our model and data. And in Section 7, we estimate our model coefficients based on TBI data and test the robustness of our model.

5.1. Traumatic brain injury

Traumatic brain injury is a leading cause of death in the United States. Each year, about two million Americans are affected by a TBI. Due to this injury, there were approximately 61,000 deaths in the United States in 2019. One of the main difficulties while diagnosing and treating traumatic brain injuries is the high level of heterogeneity in symptoms and baseline conditions among patients. Ideally, the best way to treat a TBI is by employing individualized therapy [57]. However, polytrauma patients with concomitant TBIs create an additional challenge for physicians depending on the other trauma's magnitude and severity. Additionally, unless emergency surgery is needed, these patients cannot be directly sent to the operating room (OR) since the brain needs to stabilize before doctors evaluate additional therapies. Therefore, TBI patients with additional traumas should be continuously monitored before being sent to the OR. Such circumstance creates a scheduling challenge for neurosurgeons in deciding when to send a patient to an OR to undergo a non-cranial surgery. The neurologic stability of a patient is evaluated daily by assessing dynamics in the patient's three prognostic scores, namely, the Glasgow Coma Scale (GCS), head computed tomography (CT) scan, and tiers of intracranial pressure (ICP) management. Finding the optimal scheduling time is essential because delaying non-cranial surgeries may lead to poor outcomes for polytrauma patients, while sending patients early may cause catastrophic neurological complications [57–59].

5.2. Data

Our data covers polytrauma patients with concomitant TBI who were admitted to a large hospital in the Tampa Bay region between July 2016 and December 2017. Each patient was sent to an intensive care unit (ICU). In the ICU, a trauma service was a patient's primary care team, while a neurology department consulted the trauma service about each patient's stability.

Overall, our dataset consists of 48 patient histories. We have observations on the three prognostic scores for each patient, i.e., Glasgow Coma Scale (GCS), a tier of intracranial pressure, and head computed tomography, recorded daily from the day of admission. Our data includes the patient's age, the Injury Severity Score (ISS), an urgency indicator for non-cranial surgery, and the discharge disposition. Each patient's neurologic stability was assessed and recorded daily by noting dynamics, i.e., worsening, improvement, or stability in the patient's GCS, the tier of ICP, and head CT scan. Each of the prognostic neurological scores has its scale. GCS ranges between 3 and 15 (low to high), ICP ranges between 0 (best) and 5 (worst), and CT ranges from 1 (best) to 5 (worst). Based on the three observed prognostic scores, a physician makes a daily decision about a patient's stability within the next 24 h to undergo a non-cranial surgery. Fig. 2 graphically shows our data's sequential nature for one patient released after four days in the neurological department. A neurosurgeon has two possible decisions each day (release or not release), based on the incoming information, i.e., the three neurological scores and cost associated with other trauma.

A neurosurgeon evaluates a patient every day and needs to clear them before non-cranial surgery can be performed. We refer to a day when the neurosurgeon pronounces the upcoming availability as the actual clearance. However, each clearance recommendation is difficult for a physician because of the underlying uncertainty in detecting the symptoms compounded with concomitant conditions. Hence, it is quite common for neurosurgeons to wait longer (more than possibly necessary) to assure themselves of a patient's brain's stability. To see whether a patient could have been cleared on an earlier day, a team of neurosurgeons performed a retrospective review of patients' charts to assess the earliest possible day when a patient could have been cleared for surgery. We refer to this day as the "theoretical clearance" and consider this binary variable (where 0 means *not theoretically cleared* and 1 means *theoretically cleared*) as the latent state indicator at model training.

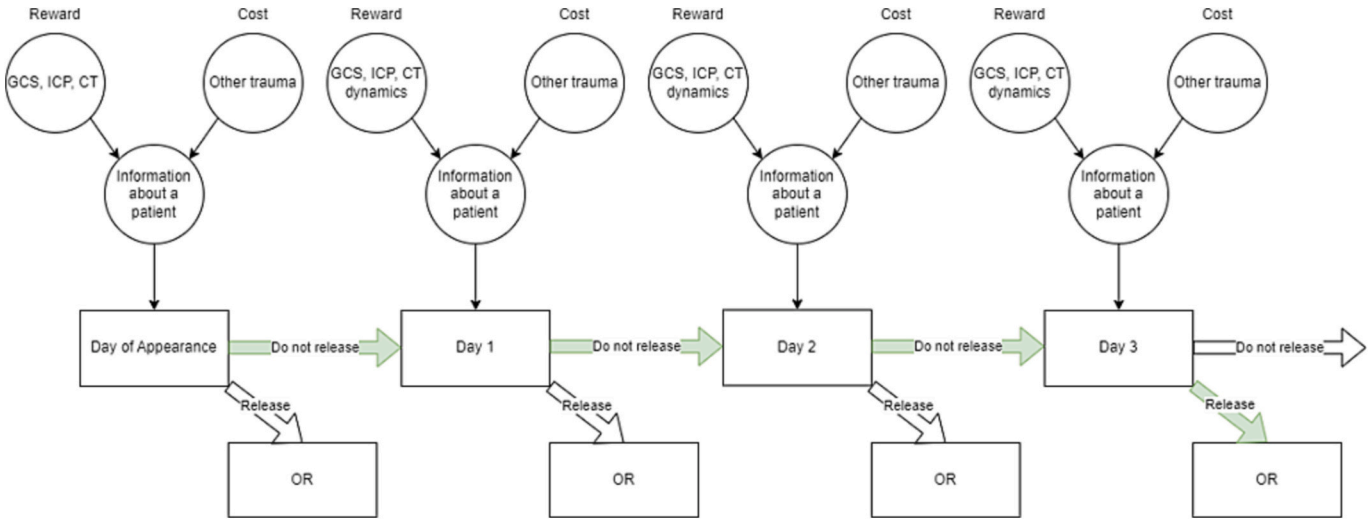

Fig. 2. Sequence of decisions.

Table 1 presents the descriptive statistics of our data. GCS, ICP, and CT at appearance are the corresponding score values when patients arrive in the hospital. GCS, ICP, and CT at clearance = 0 are the corresponding score values when patients were not theoretically cleared (i.e., theoretical clearance = 0). In contrast, GCS, ICP, and CT at clearance = 1 are corresponding score values when patients were theoretically cleared (i.e., theoretical clearance = 1). The mean age of our sample is 41 years old.

Most of the patients appeared at the hospital with an average ISS score of 26 on the scale, which ranges from 0 (no injury) to 75 (unsurvivable). The most noticeable difference between mean scores in the two states of theoretical clearance is in the GCS score (7.84 for not cleared and 9.43 for cleared patients). It is followed by the ICP score (1.42 and 1, respectively). The following example better illustrates the two states of theoretical clearance and how we calculate the means for those states. Say a patient has been cleared theoretically on day five after admission. Then, we consider the patient to be in a "not cleared" state on days one through four, and the patient's scores on these days are used to calculate mean scores for the "not cleared" state. In turn, day five is when the patient moves from the "not cleared" to a "cleared" state, and the scores on the day are used in the calculation of mean scores for the "cleared" state. The average number of days in the neurosurgical department equals 9.27 days. Its standard deviation is equal to nine, indicating high heterogeneity/overdispersion levels limiting the applicability of standard Poisson regressions in our analysis.

5.3. Applying fHMM for optimal clearing of TBI patients

Our initial task is to find the optimal speed with which polytrauma patients with concomitant TBI can safely be sent to the OR. On the one hand, Sviri, Aaslid, Douville, Moore and Newell [57] found that a physician who wants to minimize potential harm from a non-cranial surgery should wait and, ultimately, never allow a patient to undergo additional or non-cranial surgery. On the other hand, delaying surgery for the remaining traumas can lessen the chances for recovery from those additional injuries. This creates an optimal stopping problem. A neurosurgeon should find the optimal trade-off between two rewards, the reward from earlier release for the OR, and the reward from later signing off from the neurosurgical department.

Table 1
Descriptive statistics.

Variable	Mean	Median	SD	Min	Max
Age	41	36	18.49	8	85
ISS	26	24	12.12	5	66
GCS at appearance	9.88	10	3.98	3	15
ICP at appearance	0.9375	0	1.29	0	4
CT at appearance	2.04	2	0.71	1	5
Days seen by neurosurgery	9.27	5.5	8.96	1	41
GCS at clearance = 0	7.84	7	4.27	3	15
ICP at clearance = 0	1.42	2	1.24	0	4
CT at clearance = 0	2.13	2	0.62	1	5
GCS at clearance = 1	9.43	10	3.91	3	15
ICP at clearance = 1	1	0	1.26	0	4
CT at clearance = 1	1.95	2	0.62	1	5

A doctor has a finite set of policies, $A = \{Keep, Release\}$ at each point in time. The observed information is the sequence of prognostic neurological scores, GCS, ICP, and CT, and prognostic information recorded at admission time, the ISS score, and age. The finite set of observable states is $S = \{Not\ Stable, Stable\}$. At each time point, a doctor's objective is to track the state of a patient, given the observed information about the patient. The state "Stable" is absorbing, which means the prediction stops as soon as it happens. A doctor is uncertain about the true condition of a patient. Still, the doctor may infer this information using the observable values of the prognostic scores and release the patient as soon as they are certain by applying a sequence of policies π from the finite alphabet A to maximize $R(S_t, a_t)$. At the same time, the doctor wants to minimize costs $C(S_t, a_t)$ by applying the same sequence of policies π and find $V_\pi^* = \max_\pi V_\pi = \max_\pi (R_\pi(S_t, a_t) - C_\pi(S_t, a_t))$.

One unique feature of this example is the intrinsic reward and cost functions. Ordinarily, either functional form or units of measure are known for reward and cost function. However, this is not a case in our setting. Thus, we relax those assumptions and use a parametric approximation (estimated from the data) to decompose cost and reward functions. To decompose those functions in our study, we apply the following logic. Since the theoretical clearance is the revision of histories in which doctors accounted for both the neurological stability and the conditions of other types of traumas, we consider the first day when a patient is theoretically cleared as the best combination of the reward and the cost functions.

Let us assume that we observe a population of patients with no TBI but only traumas like our TBI patients' and record non-cranial surgeries conducted at different times. Comparing the outcomes for patients with similar trauma severity, but at other time points, we could figure out the cost of performing surgery later rather than sooner. Assuming that immediate surgery offers the maximum value (the best combination of reward and cost) and that after some time, the surgery becomes useless

(the maximum cost), we can project the cost on a range from zero to one. We may use a cumulative distribution function of time as a proxy for the cost function, e.g., a Weibull distribution that can take various shapes and is widely used to analyze time to failure.

To measure rewards, we use the probability to be cleared solely based on the neurological scores to measure certainty about the patient's brain stability. Again, the probability is in the range from zero to one. Summing up these two numbers and maximizing over the set of sequences of possible policies, we obtain the best policy sequence for each patient.

Fig. A.1.9a in the Online Appendix A shows the mathematical form of our final model. Here, $\nabla y_{ijt} = y_{ijt} - y_{ij(t-1)}$ is the daily change in score j, $j = [GCS, ICP, CT]$, for patient i. $\left\{\nabla y_{ijT}\right\}_{T=t-4}^{t}$ is a vector of length five containing the last five changes, i.e., starting from five days prior. In this example, we use the neurosurgeons' logic and keep only the last five changes of the scores. Thus, it is possible to use the regression approach to track a function of observations where X_{iK} is a vector of the covariates. We assume that the cost grows with a constant rate ρ_i. This is individually calculated for each patient i based on the initial prognostic scores, the ISS score, and the patient's age. Our rationale behind this assumption is that the trauma other than TBI is constant over time unless repaired during a non-cranial surgery. Thus, the future benefits of the surgery are decreasing over time. We also assume that rewards are related to the probability of being cleared. This probability can be seen as the certainty about the patient's stability, and its increase can be seen as reducing the doctor's uncertainty. Consequently, if a doctor releases a stable patient, they get the maximum possible rewards for that. Fig. A.1.9b demonstrates the interaction version of our model (referred to as fHMM-int). The only difference between the basic fHMM and fHMM-int is the interactions between ISS and three neurological scores in the equation for the growth rate. We add the interaction because, as ISS is the combination of all patient's traumas, the same severity on ISS score can be reached due to other trauma, brain trauma, or both.

6. Simulation study

Before estimating our model based on real data, we perform simulations to show that our method can indeed recover the true parameters. We simulate GCS, ICP, and CT scores and the probabilities to be cleared for ten hypothetical patients for 14 days. We use the code in Fig. A.1.1 in Online Appendix A to this article to simulate neurological scores. We use the descriptive statistics shown in Subsection 5.2 to simulate scores on the day of appearance. We sample from prior distributions for each model parameter to simulate paths and recover the whole path for each hypothetical patient. The results are shown in Fig. A.1.10 in the Online Appendix A.

In the top left panel of Fig. A.1.10, we plot simulated GCS scores for ten hypothetical patients. The dynamic is positive for most patients, indicating that brain stability increases with time. We see two patients whose GCS was high initially and started decreasing with time. Since we simulate data for 14 days, it is unlikely that patients with such high GCS scores will stay so long. It is possible only when GCS starts decreasing, indicating instability of a patient's brain. Hence, our model can articulate such a scenario. In the top right panel and the bottom left panel of Fig. A.1.10, we plot simulated ICP and CT scores for the same ten hypothetical patients, respectively. Several simulated patients have ICP and CT scores that do not change or worsen with time. It may be a possibility for patients with severe brain injuries. In this case, patients may have extensive hematomas that may grow with time, declining CT and ICP scores. The total probability of releasing the patients, plotted in the bottom right panel of Fig. A.1.10, increases as well. However, we observe inflection points on most of the probabilities of someday. It aligns with the fact that after someday, the improvement in brain stability is offset by the negative effect of time on the other trauma. We can see that all three scores primarily either improve or do not change with time. This fact aligns with the previous research on TBI patients, concluding that a brain fixes itself with time Sviri, Aaslid, Douville, Moore and Newell [57]. Another observation is that patients with poorer scores are less likely to be released, which also aligns with the practice when neurosurgeons wait longer to release patients with less favorable brain conditions.

7. Estimating fHMM for TBI patients and robustness checks

7.1. Estimating the fHMM

We estimate the model (Fig. 2) using the *rstan*[1] package for *R* [60]. (The complete R code along with data for the model can be found in the Online Appendix A to this article.) We run three chains with 10,000 iterations and 3000 burn-in iterations. After running the model with default settings, we receive a warning regarding divergent transitions after burn-in. Following recommendations in *Stan's users documentation,*[2] we increase the adaptation delta parameter, responsible for the target average acceptance rate, to 0.9. And the final adjustment to the default settings is the step size parameter. This parameter sets the initial step size from which the algorithm begins. It is recommended to set it smaller for complicated problems to facilitate adaptation. We set it equal to 0.5.

Table A.1.1 shows the estimated coefficients. We can see two significant parameters in the negative binomial regression, δ_1^{ICP} and δ_1^{GCS}. These imply that each additional point in ICP corresponds to a 25% increase, and each additional point in GCS corresponds to a 10% decrease in the expected number of days in the neurosurgical department, keeping all other variables constant. For the cost function, we find ISS and CT β_ρ^{ISS} and β_ρ^{CT} also to be significant. Both increase the scale parameter of the cost function. That means that the higher ISS and CT, the slower the cost function grows, keeping all other parameters the same. The value of $\lambda = 4.86$ indicates that the cost rises with time, i.e., it is less beneficial to keep a patient longer.

There are several significant coefficients in the equations tracking the functional change in the GCS, ICP, and CT. All the $\beta_1^{'}s$ coefficients are significant, indicating the importance of today's scores to predict tomorrow's scores. For CT, yesterday's changes (β_{22}^{CT}), and changes three days ago (β_{24}^{CT}) are significant and positive. That indicates that the positive changes (decrease in the score) on those days make our expectation for tomorrow's CT score more positive (lower CT score). Also, β_{24}^{ICP} and β_{25}^{ICP} are significant and positive, indicating the importance of historical changes in both ICP scores. It also means that the positive changes (decrease in the score) on those days make our expectation for tomorrow's ICP score more positive (that it will show a lower ICP score).

When estimating the probability of being released and the rewards function, we find that the current GCS and ICP scores, the previous day's probability of being released, and the current cost related to the other trauma are significant predictors of today's chance of being released. One unit increase in GCS increases the odds of being released by 850%, and one unit increase in ICP decreases the odds of being released by 99%. The coefficient for the probability on the previous day, ϑ_4, indicates that a 0.1 unit increase in the probability on the previous day increases current day odds by 41% while keeping all other parameters constant.

We also find α_1 to be positive and statistically significant. That means the higher probability of being released corresponds to the higher rewards.

Finally, we want to discuss the forward-looking coefficients, i.e., $\vartheta_1^{GCS}, \vartheta_1^{ICP}, \vartheta_1^{CT}$ from Table A.1.1 in the Online Appendix A. As one can

[1] Stan Development Team, RStan: the R interface to Stan. R package version 2.21.2, 2020. http://mc-stan.org/.

[2] Stan Development Team, Runtime warnings and convergence https://mc-stan.org/misc/warnings.html#divergent-transitions-after-warmup, 2022.

see, both 90% and 95% credibility intervals for all the coefficients include zero. The absence of statistical significance means that not all physicians appear to be forward-looking, but value based on the just past dynamics of the prognostic scores. In other words, physicians are heterogeneous in their preferences towards the value of the future. This fact also finds support in Table A.1.2 of the Online Appendix A. Looking at the results for bootstrapping, the 95% confidence intervals for those parameters are wide. That means that given different samples, we may have mostly those who value the future or vice versa.

7.2. Robustness check

In Table 2, we compare two versions of our model, fHMM (Model 5) and fHMM with interactions (Model 6), with four alternative specifications: a logit model (Model 1), a generalized additive model (GAM) (Model 2), POMDP (Model 3), and the model developed by McCallum, Freitag and Pereira [51] (Model 4).

As covariates for the logit model, we use GCS, ICP, and CT scores observed on the day of making a prediction, the day of the patient's hospital stay, and age. For the generalized additive model, we train a spline with five knots and the same predictors as for the logistic regression. As for POMDP, since it is a time-series model, we consider the clearance decision a latent state, the current day GCS, ICP, and CT scores as the observations conditioned on the latent state, and the patient's age as a covariate. We convey the time dependency by conditioning the current latent state on each patient's previous day latent state. McCallum's model is an extension to POMDP, except that the current latent state is conditioned on the previous day latent state and the current observations.

We use the *rstan* package in *R* as before to estimate Models 3 and 4. As before, we run three chains with 10,000 iterations with 3000 warm-up iterations for each model. We use an adaptation delta of 0.9, a maximum tree depth of 10, and a step size of 0.5. To program Model 1 and Model 2, we use standard R functions, *glm()* and *gam()*.

We compare models based on their information criterion. For both logit and GAM models, we provide the Akaine Information Criterion (AIC). In contrast, for POMDP, McCallum, and both versions of our model, we provide leave-one-out information criteria (LOOIC) typically used for comparing Markov Chain Monte Carlo models. The idea of the leave-one-out information criteria is similar to AIC by estimating the predictive log density of a new dataset and can be used in the same manner as AIC to compare a MCMC model to a frequentist model [61]. However, the difference is that AIC ignores the contribution of the prior distributions and assumes the posterior distributions to be multivariate normal. To calculate the log-likelihood in stan, we create a separate vector containing pointwise log-likelihood and use the *loo()* function from the *rstan* package.

The results are shown in Table 2. We can see that the logit and GAM models have the worst fit (i.e., highest values of the information criterion) among the six models. All four Bayesian models outperform the frequentist models. Among them, both versions of our model show the best performance (with Model 6 being the best), and McCallum's model outperforms POMDP. One of the reasons is that, unlike POMDP where observations are conditioned on hidden states, McCallum conditions hidden states on observations. In situations like ours, we predict a state sequence given an observation sequence. In addition, due to the small sample size, it is easier to train a conditional model like McCallum's see [33] because we do not need to account for the effect of the feedback from states on the posterior distributions of observations.

Given the small sample size, we conduct a bootstrapping procedure (also called "subsampling") [62] to check the validity of coefficient estimates. We choose resampling with replacement as a bootstrapping method and run our model 50 times. The code for bootstrapping is shown in Fig. A.1.2 in the Online Appendix A for this article. The bootstrapping procedure is implemented in the *transformed parameters* block. If *resample* in the list with data is set to 1, Fig. A.1.6 in the Online Appendix A, we randomly choose 48 patients with replacements from the initial dataset each time we run the model. We do this procedure 50 times, i.e., using 50 different samples of 48 patients with replacement and fitting the model for each sample. Then, we calculate a summary statistic for each bootstrap iteration and construct a sample of means. We use this sample to build 95% confidence intervals for each coefficient in our model.

Since some of our model's bootstrap distributions of parameters are not symmetric (see Fig. A.1.8 in the Online Appendix A), we apply a bias-corrected method to obtain more reliable bootstrap confidence intervals [63]. The results of the bootstrapping procedure are presented in Table A.1.2. As one can see from the last column of the table, all original estimates except β_{25}^{CT} and α_1 are inside 95% confidence intervals for the corresponding parameter estimator distributions.

These results prove that our model is robust to small samples, and doctors can apply it for decision-making. In the next section, we discuss the managerial implications of our model.

7.3. Precision assessment

Next, we compare the utility of our models to other models and actual decisions. First, Table 3 compares the four Bayesian and neural network models. We have decided to add the latter to compare how the Bayesian models can compete with neural networks in such complex environments. For the neural network model, we use daily GCS, ICP, and CT readings as input, and the neurosurgeon's clearance decision on the corresponding day as output. We also wanted to add recurrent neural networks (RNN) for comparison since it seems very similar to the model we develop in this paper; however, we encountered several limitations of RNN for our case (see Online Appendix C for a comparison). The first column contains differences in expected log pointwise predictive density (ELPD) between the corresponding model and fHMM-int. The numbers in parentheses for POMDP and McCallum's model show the difference in ELPD between fHMM and the corresponding model. ELPD shows how close the predictions of a model are to the true data [61]. The negative numbers indicate that fHMM with interactions is preferred over all other models. Negative numbers in parentheses show that fHMM is preferred

Table 2
Model comparison.

Model #	Model name	Short model description	Information criterion
1	Logit	Ignore dynamics and latent states	392.73
2	GAM	As logit but accounting for score dynamics	316.43
3	POMDP	Using the last day observation in an optimal stopping formulation	315.4
4	McCallum et al.	As POMDP but reverse dependency between current latent state and current observation	260.4
5	fHMM	Using the full dynamics of scores	240.7
6	fHMM-int	As fHMM but with interactions in a cost function	225.5

Table 3
Bayesian models and actual decision comparison (threshold = 0.5).

Model	ELPD difference	SE difference	Exact predictions	Early predictions	Late predictions
fHMM-int	0.0	0.0	18	10	20
fHMM	−5.8 (0.0)	3.7 (0.0)	22	11	15
McCallum et al.	−18.8 (−8.4)	5.1 (2.7)	20	14	14
POMDP	−64.1 (−36.1)	5.8 (5.7)	20	15	13
Neural Network	NA	NA	43	2	3

over two other models. The second column (SE difference) contains the standard error of differences in ELPD between the corresponding model and fHMM with interactions. Again, numbers in parentheses show the SE difference between fHMM and two other models. We can see that the 95% posterior confidence interval does not cover "zero" concerning both the McCallum and POMDP alternatives. This suggests that fHMM is significantly better than the two other models.

The last three columns show the number of exact, early, and late predictions. Our models decide to release a patient if their predicted probability of release exceeds a certain threshold; here and further in the paper, we use a naïve threshold of 0.5. We compare our models' predicted day of release with the day of theoretical clearance. An exact prediction is where a model correctly predicts the day of theoretical clearance. Early predictions correspond to patients the model releases earlier than the day of theoretical clearance. And late predictions correspond to those patients which the model releases later than the day of theoretical clearance. The day of theoretical clearance reflects a doctor's decision after reviewing a history of observations, at which point there is no uncertainty about the future. This is in contrast to their actual decision, which is made in circumstances of uncertainty about the patient's future brain stability. Because the day of theoretical clearance is the earliest release day for each patient, if a model releases a patient earlier than the day of theoretical clearance, there is a high chance of the patient's death during a non-cranial surgery. Hence, late predictions are safer (i.e., less expensive) than early ones. The cost of the late prediction is the amount of money needed to observe a patient in ICU plus the possible decrease in outcome for a non-cranial surgery. In contrast, the potential cost of an early prediction is infinite (i.e., death). Thus, our primary focus will be on reducing the number of early predictions while maximizing exact predictions.

Considering columns 4–6 in Table 3, fHMM produces the highest number of exact predictions. It also has the fewest number of early predictions. In fact, fHMM increases the number of exact predictions by 10% and decreases the number of early predictions by 21.4% compared to McCallum. Due to the overwhelming outperformance of the Bayesian models, we remove the neural network model from further consideration.

Table 4 compares different types of predictions by ISS category for three different thresholds. Originally, ISS was the continuous score ranging from 0 to 75. Bolorunduro, Villegas, Oyetunji, Haut, Stevens, Chang, Cornwell III, Efron and Haider [64] suggests the following categories of ISS: minor (less than 9), moderate (9–15), severe (16–24), and profound (greater than 25). In our sample of 48 patients, we have two patients in the *Minor* category, five in the *Moderate* category, 19 in the *Severe* category, and 22 in the *Profound* category. In Table 4, we compute the exact early and late predictions using the naïve threshold of 0.5; then, we compare it to additional thresholds of 0.75 and 0.8. We first discuss the result for a threshold of 0.5.

From Table 4, we see that three models have the same predictions for minor and moderate categories. We start noticing differences in the severe category. In this category, fHMM has the same number of exact predictions as McCallum et al. and fHMM with interactions (fHMM interactions in the Table 4) but fewer early predictions. fHMM outperforms POMDP for the severe category by one exact prediction and two early predictions. fHMM also performs better for the most complex category, the profound category: it outperforms fHmm with interactions, McCallum et al. McCallum, Freitag and Pereira [51] and POMDP by four, two and one exact prediction, respectively. It also makes a smaller number of early predictions than McCallum et al. McCallum, Freitag and Pereira [51] and POMDP but more than fHMM

Table 4
Bayesian model comparison by patients' category of ISS for three thresholds (0.5, 0.75 and 0.8).

			ISS category			
Prediction type	Model	Threshold	*Minor*	*Moderate*	*Severe*	*Profound*
Early Predictions	fHMM-int	*0.5*	0	2	4	4
		0.75	0	2	1	2
		0.8	0	2	1	2
	fHMM	*0.5*	0	2	3	6
		0.75	0	0	1	2
		0.8	0	0	0	0
	McCallum et al.	*0.5*	0	2	4	8
		0.75	0	0	0	1
		0.8	0	0	0	1
	POMDP	*0.5*	0	2	5	8
		0.75	0	0	0	0
		0.8	0	0	0	0
Exact Predictions	fHMM-int	*0.5*	0	2	10	6
		0.75	0	1	7	1
		0.8	0	1	6	1
	fHMM	*0.5*	0	2	10	10
		0.75	0	3	5	2
		0.8	0	3	5	3
	McCallum et al.	*0.5*	0	2	10	8
		0.75	0	2	4	4
		0.8	0	2	4	2
	POMDP	*0.5*	0	2	9	9
		0.75	0	0	0	1
		0.8	0	0	0	0
Late Predictions	fHMM-int	*0.5*	2	1	5	12
		0.75	2	2	11	19
		0.8	2	2	12	19
	fHMM	*0.5*	2	1	6	6
		0.75	2	2	13	18
		0.8	2	2	14	19
	McCallum et al.	*0.5*	2	1	5	6
		0.75	2	3	15	17
		0.8	2	3	15	19
	POMDP	*0.5*	2	1	5	5
		0.75	2	5	19	21
		0.8	2	5	19	22

with interactions.

In addition to the above naïve threshold of 0.5, we also apply thresholds of 0.75 and 0.8 (see e.g., lines two and three in Table 4). The results suggest that the optimal threshold is 0.8. For that threshold, fHMM has no early predictions and has the highest number of exact predictions.

As mentioned earlier, a physician's actual clearance is usually later than their theoretical (i.e., post hoc revised) clearance. Fig. A.1.7 (Online Appendix) presents three patients' estimated release probabilities over time. The actual clearance for each patient happens on the last day. The day of theoretical clearance is shown with a green vertical line. One can see that the theoretical clearance happens when the estimated probability is around 60%. Thus, hospital doctors may apply our analysis results to decision-making in the following manner. As soon as, according to the model, the patient's predicted probability of being released reaches a 60% threshold, doctors can be confident to release such a patient on the current day.

Table 5 compares fHMM (using again thresholds of 0.5, 0.75, and 0.8), fHMM with interactions and the actual decision by neurosurgeons. For a threshold of 0.5, we can see that fHMM has more exact predictions and fewer late predictions, and fHMM with interactions has the same number of exact predictions and fewer late predictions compared to a physician's actual decision. In fact, fHMM shows a 22.2% increase in the total number of exact predictions and a 34.8% decrease in the total number of late predictions, while fHMM with interactions shows 13.3% decrease in the total number of late predictions. fHMM has the same number of early predictions: three in the *Severe* ISS category. We also see that most early predictions for fHMM happen at the *Profound* category, six. This category is where our model produces the highest number of early predictions compared to the actual decision, six versus one. However, when increasing the threshold from 0.5 to 0.8, the number of early predictions reduce to zero.

On the other hand, fHMM with interactions has less early predictions for *Profound* category, four, but one more early prediction in the *Severe* category than fHMM. However, increasing the threshold does not help to reduce the number of early predictions to zero. From Table 4, at this threshold, McCallum et al. McCallum, Freitag and Pereira [51] still has one early prediction for the *Profound* category. From the same table, POMDP does not have any early predictions at this threshold level, but it also has no exact predictions while fHMM has 11 exact predictions.

Table 6 compares the same models on how many days are saved for patients who have been released in accordance with or later than the day of theoretical clearance, and on average savings per patient. Online Appendix B describes how we conducted our calculations. In short, the fHMM highlights the potential for the most cost-saving per patient compared with the relevant benchmarks.

Table 6
Performance comparison (threshold = 0.5).

Model	TBI severity	Number of patients (Exact + Late)	Total difference in days	Average savings per patient
fHMM	GCS ≥13	15	17	$3955
	9 ≤GCS ≤12	8	2	$969
	GCS ≤8	14	81	$27,546
fHMM-int	GCS ≥13	15	16	$3723
	9 ≤GCS ≤12	9	2	$861
	GCS ≤8	14	80	$27,206
McCallum et al.	GCS ≥13	12	17	$4944
	9 ≤GCS ≤12	7	2	$1107
	GCS ≤8	14	69	$23,465
POMDP	GCS ≥13	12	17	$4944
	9 ≤GCS ≤12	8	2	$969
	GCS ≤8	14	67	$22,785

8. Discussion and implications

In this study, we present a novel framework aimed at integrating dynamic variables into optimal stopping problems. While this approach has the potential to facilitate more personalized decision-making and account for patient heterogeneity, it also comes with its own set of limitations. Specifically, the choice of smoothing techniques and the level of smoothing can significantly impact the reliability of the model's estimated hidden states. Moreover, the integration of velocity data could add another layer of complexity, necessitating careful parameterization and assumptions.

The implications of our research could be particularly meaningful for healthcare professionals involved in traumatic brain injury (TBI) treatment. For instance, elevated levels of intracranial pressure (ICP) and head CT scores may suggest that the focus should be on brain recovery rather than treating other forms of trauma. Similarly, initial Glasgow Coma Scale and ICP scores can offer insights into the likely length of a

Table 5
Comparison of fHMM and actual decision by patients' category of ISS for three thresholds (0.5, 0.75 and 0.8).

			ISS category			
Prediction type	Model	Threshold	*Minor*	*Moderate*	*Severe*	*Profound*
Early Predictions	fHMM-int	*0.5*	0	2	4	4
		0.75	0	2	1	2
		0.8	0	2	1	2
	fHMM	*0.5*	0	2	3	6
		0.75	0	0	1	2
		0.8	0	0	0	0
	Actual Decision		1	2	3	1
Exact Predictions	fHMM-int	*0.5*	0	2	10	6
		0.75	0	1	7	1
		0.8	0	1	6	1
	fHMM	*0.5*	0	2	10	10
		0.75	0	3	5	2
		0.8	0	3	5	3
	Actual Decision		1	0	7	10
Late Predictions	fHMM-int	*0.5*	2	1	5	12
		0.75	2	2	11	19
		0.8	2	2	12	19
	fHMM	*0.5*	2	1	6	6
		0.75	2	2	13	18
		0.8	0	2	14	19
	Actual Decision		0	3	9	11

patient's stay in the neurosurgical department. This information could prove valuable for hospital resource planning.

Our findings may also assist clinicians during the patient discharge process. Specifically, current CT scores and the previous day's probability of release could serve as key variables in deciding whether a patient is ready for discharge. With increased application across healthcare settings, the model has the potential to gather more case-specific data, thereby refining its predictive capabilities. A mobile application offering real-time release probabilities based on current patient data could serve as a practical extension of our model, intended to augment, not replace, clinicians' expert judgment [65–68].

We acknowledge our study's limitations, such as its small sample size and the consequent need for broader research to generalize our findings. Future research could explore the application of this model in diverse healthcare environments, as well as consider variables like individual neurosurgeon expertise and potential evaluation biases. However, despite these limitations, our model offers preliminary insights into improving collaborative decision-making among medical professionals by leveraging variability in clinical expectations.

Building on feedback from referees, we see potential for our approach to be adapted for different medical scenarios and healthcare units, such as emergency orthopedic units dealing with compound fractures. Our current data smoothing approach is tailored to our small dataset but could potentially be modified to suit larger, more diverse data sets in these other medical contexts.

In summary, our study presents a specialized healthcare decision-making framework that incorporates dynamic state variables into Hidden Markov Models (HMMs). Our empirical findings underscore the potential influence of dynamically collected prognostic scores on patient outcomes and resource allocation. Although further validation is needed, our work holds promise for enriching both academic research and practical applications in ICU settings.

CRediT authorship contribution statement

Gleb Zavadskiy: Data curation, Conceptualization, Formal analysis, Methodology, Software, Writing – original draft, Writing – review & editing. **Daniel Zantedeschi:** Conceptualization, Methodology, Validation, Writing – review & editing, Project administration. **Wolfgang Jank:** Conceptualization, Methodology, Formal analysis, Validation, Writing – review & editing.

Declaration of Competing Interest

The authors declare that they have no known competing financial interests or personal relationships that could have appeared to influence the work reported in this paper.

Data availability

We do not have persmission to share the data. We plan to share the code and simulations to favor adoption and reproducibility.

Appendix. Supplementary data

Supplementary data to this article can be found online at https://doi.org/10.1016/j.dss.2023.114078.

References

[1] D. Barrera Ferro, S. Brailsford, C. Bravo, H. Smith, Improving healthcare access management by predicting patient no-show behaviour, Decis. Support. Syst. 138 (2020) 113398.

[2] J. Fredrickson, M. Mannino, O. Alqahtani, F. Banaei-Kashani, Using similarity measures for medical event sequences to predict mortality in trauma patients, Decis. Support. Syst. 116 (2019) 35–47.

[3] S. Adeyemi, E. Demir, T. Chaussalet, Towards an evidence-based decision making healthcare system management: modelling patient pathways to improve clinical outcomes, Decis. Support. Syst. 55 (1) (2013) 117–125.

[4] G.J. Browne, E.A. Walden, Stopping information search: an fMRI investigation, Decis. Support. Syst. 143 (2021), 113498.

[5] P. Jiang, X. Liu, J. Zhang, X. Yuan, A framework based on hidden Markov model with adaptive weighting for microcystin forecasting and early-warning, Decis. Support. Syst. 84 (2016) 89–103.

[6] X. Li, Y. Zhuang, B. Lu, G. Chen, A multi-stage hidden Markov model of customer repurchase motivation in online shopping, Decis. Support. Syst. 120 (2019) 72–80.

[7] A. Moayedikia, H. Ghaderi, W. Yeoh, Optimizing microtask assignment on crowdsourcing platforms using Markov chain Monte Carlo, Decis. Support. Syst. 139 (2020), 113404.

[8] Y. Zak, A. Even, Development and evaluation of a continuous-time Markov chain model for detecting and handling data currency declines, Decis. Support. Syst. 103 (2017) 82–93.

[9] S. Chick, M. Forster, P. Pertile, A Bayesian decision-theoretic model of sequential experimentation with delayed response, J. R. Stat. Soc. Ser. B 79 (5) (2017) 1439–1462.

[10] P. Pertile, M. Forster, D. La Torre, Optimal Bayesian sequential sampling rules for the economic evaluation of health technologies, J. R. Stat. Soc. Ser. A (Stat. Soc.) 177 (2) (2014) 419–438.

[11] F. de Mello-Sampayo, On the timing and probability of presurgical teledermatology: how it becomes the dominant strategy, Health Care Manag. Sci. (2022) 1–17.

[12] A. Diamant, Dynamic multistage scheduling for patient-centered care plans, Health Care Manag. Sci. 24 (4) (2021) 827–844.

[13] A.J. Culyer, Y. Bombard, An equity framework for health technology assessments, Med. Decis. Mak. 32 (3) (2012) 428–441.

[14] T. Ayer, O. Alagoz, N.K. Stout, OR forum—a POMDP approach to personalize mammography screening decisions, Oper. Res. 60 (5) (2012) 1019–1034.

[15] A. Boloori, S. Saghafian, H.A. Chakkera, C.B. Cook, Data-driven management of post-transplant medications: an ambiguous partially observable markov decision process approach, Manuf. Serv. Oper. Manag. 22 (5) (2020) 1066–1087.

[16] M.R. Skandari, S.M. Shechter, Patient-type Bayes-adaptive treatment plans, Oper. Res. 69 (2) (2021) 574–598.

[17] O. Alagoz, H. Hsu, A.J. Schaefer, M.S. Roberts, Markov decision processes: a tool for sequential decision making under uncertainty, Med. Decis. Mak. 30 (4) (2010) 474–483.

[18] C. Excellence, Guide to the Methods of Technology Appraisal 2013 [Internet], 2013.

[19] S. Boyarchenko, S. Levendorskii, Irreversible Decisions under Uncertainty: Optimal Stopping Made Easy, Springer Science & Business Media, 2007.

[20] A. Petropoulos, S.P. Chatzis, S. Xanthopoulos, A hidden Markov model with dependence jumps for predictive modeling of multidimensional time-series, Inf. Sci. 412 (2017) 50–66.

[21] S.L. Scott, G.M. James, C.A. Sugar, Hidden Markov models for longitudinal comparisons, J. Am. Stat. Assoc. 100 (470) (2005) 359–369.

[22] M.J. Zaki, C.D. Carothers, B.K. Szymanski, VOGUE: a variable order hidden markov model with duration based on frequent sequence mining, ACM Trans. Knowl. Discov. Data (TKDD) 4 (1) (2010) 5.

[23] S. Ayabakan, I. Bardhan, E. Zheng, What drives patient readmissions? A new perspective from the hidden Markov model analysis, in: International Conference on Information Systems, 2016. Dublin.

[24] L. Yan, Y. Tan, Feeling blue? Go online: an empirical study of social support among patients, Inf. Syst. Res. 25 (4) (2014) 690–709.

[25] V. Krishnamurthy, Partially Observed Markov Decision Processes, Cambridge university press, 2016.

[26] L.B. Hartman, K.M. van Hee, Application of Markov decision processes to search problems, Decis. Support. Syst. 14 (3) (1995) 283–298.

[27] S. Voorberg, R. Eshuis, W. van Jaarsveld, G.J. van Houtum, Decisions for information or information for decisions? Optimizing information gathering in decision-intensive processes, Decis. Support. Syst. 151 (2021), 113632.

[28] M. Cevik, T. Ayer, O. Alagoz, B.L. Sprague, Analysis of mammography screening policies under resource constraints, Prod. Oper. Manag. 27 (5) (2018) 949–972.

[29] Q. Chen, T. Ayer, J. Chhatwal, Optimal m-switch surveillance policies for liver cancer in a hepatitis c–infected population, Oper. Res. 66 (3) (2018) 673–696.

[30] F.S. Erenay, O. Alagoz, A. Said, Optimizing colonoscopy screening for colorectal cancer prevention and surveillance, Manuf. Serv. Oper. Manag. 16 (3) (2014) 381–400.

[31] R. Ibrahim, B. Kucukyazici, V. Verter, M. Gendreau, M. Blostein, Designing personalized treatment: an application to anticoagulation therapy, Prod. Oper. Manag. 25 (5) (2016) 902–918.

[32] J. Zhang, B.T. Denton, H. Balasubramanian, N.D. Shah, B.A. Inman, Optimization of PSA screening policies: a comparison of the patient and societal perspectives, Med. Decis. Mak. 32 (2) (2012) 337–349.

[33] M. Plummer, Cuts in Bayesian graphical models, Stat. Comput. 25 (1) (2015) 37–43.

[34] P. Bühlmann, A.J. Wyner, Variable length Markov chains, Ann. Stat. 27 (2) (1999) 480–513.

[35] Z. Ghahramani, M. Jordan, Factorial hidden Markov models, Adv. Neural Inf. Proces. Syst. 8 (1995).

[36] E. Bayraktar, M. Ludkovski, Sequential tracking of a hidden Markov chain using point process observations, Stoch. Process. Appl. 119 (6) (2009) 1792–1822.

[37] E. Bayraktar, S. Sezer, Quickest detection for a poisson process with a phase-type change-time distribution, in: arXiv Preprint Math/0611563, 2006.

[38] S. Chick, M. Forster, P. Pertile, A Bayesian decision-theoretic model of sequential experimentation with delayed response, J. R. Stat. Soc. Ser. B 79 (5) (2017) 1439–1462.
[39] P. Pertile, M. Forster, D. La Torre, Optimal Bayesian sequential sampling rules for the economic evaluation of health technologies, J. R. Stat. Soc. Ser. A (Stat. Soc.) (2014) 419–438.
[40] Z. Dai, H. Yu, B.K.H. Low, P. Jaillet, Bayesian optimization meets Bayesian optimal stopping, in: International Conference on Machine Learning, PMLR, 2019, pp. 1496–1506.
[41] G. Zavadskiy, D. Zantedeschi, W. Jank, A Bayesian optimal stopping framework for traumatic brain injuries patients, in: ICIS Proceedings 2, 2021.
[42] A.J. Schaefer, M.D. Bailey, S.M. Shechter, M.S. Roberts, Modeling medical treatment using Markov decision processes, in: Operations Research and Health Care, Springer, 2005, pp. 593–612.
[43] J.C. Arango-Lasprilla, M. Rosenthal, J. DeLuca, D.X. Cifu, R. Hanks, E. Komaroff, Functional outcomes from inpatient rehabilitation after traumatic brain injury: how do Hispanics fare? Arch. Phys. Med. Rehabil. 88 (1) (2007) 11–18.
[44] S. Asgari, H. Adams, M. Kasprowicz, M. Czosnyka, P. Smielewski, A. Ercole, Feasibility of hidden Markov models for the description of time-varying physiologic state after severe traumatic brain injury, Crit. Care Med. 47 (11) (2019) e880–e885.
[45] A. Ercole, E. Thelin, A. Holst, B. Bellander, D. Nelson, Kinetics of serum S100b after traumatic brain injury, BMC Neurol. 16 (93) (2016).
[46] R.B. Myers, C. Lazaridis, C.M. Jermaine, C.S. Robertson, C.G. Rusin, Predicting intracranial pressure and brain tissue oxygen crises in patients with severe traumatic brain injury, Crit. Care Med. 44 (9) (2016) 1754–1761.
[47] M. Smits, D.W. Dippel, P.J. Nederkoorn, H.M. Dekker, P.E. Vos, D.R. Kool, D.A. van Rijssel, P.A. Hofman, A. Twijnstra, H.L. Tanghe, Minor head injury: CT-based strategies for management—a cost-effectiveness analysis, Radiology 254 (2) (2010) 532–540.
[48] E. Kırkızlar, D.M. Faissol, P.M. Griffin, J.L. Swann, Timing of testing and treatment for asymptomatic diseases, Math. Biosci. 226 (1) (2010) 28–37.
[49] L.M. Maillart, J.S. Ivy, S. Ransom, K. Diehl, Assessing dynamic breast cancer screening policies, Oper. Res. 56 (6) (2008) 1411–1427.
[50] B. Sandıkçı, L.M. Maillart, A.J. Schaefer, M.S. Roberts, Alleviating the patient's price of privacy through a partially observable waiting list, Manag. Sci. 59 (8) (2013) 1836–1854.
[51] A. McCallum, D. Freitag, F.C. Pereira, Maximum entropy Markov models for information extraction and segmentation, in: Intl. Conf. on Machine Learning, 2000, pp. 591–598.
[52] N.Z. Foutz, W. Jank, Research note—prerelease demand forecasting for motion pictures using functional shape analysis of virtual stock markets, Mark. Sci. 29 (3) (2010) 568–579.
[53] W.K. Hastings, Monte Carlo sampling methods using Markov chains and their applications, Biometrika 57 (1) (1970) 97–109.
[54] N. Metropolis, A.W. Rosenbluth, M.N. Rosenbluth, A.H. Teller, E. Teller, Equation of state calculations by fast computing machines, J. Chem. Phys. 21 (6) (1953) 1087–1092.
[55] O. Cappé, E. Moulines, T. Rydén, Inference in hidden markov models, in: Proceedings of EUSFLAT Conference, 2009, pp. 14–16.
[56] C.P. Robert, The Bayesian Choice: From Decision-Theoretic Foundations to Computational Implementation, Springer, 2007.
[57] G.E. Sviri, R. Aaslid, C.M. Douville, A. Moore, D.W. Newell, Time course for autoregulation recovery following severe traumatic brain injury, J. Neurosurg. 111 (4) (2009) 695–700.
[58] P. Curry, D. Viernes, D. Sharma, Perioperative management of traumatic brain injury, Int. J. Crit. Illn. Inj. Sci. 1 (1) (2011) 27.
[59] J. Gao, Z. Zheng, Development of prognostic models for patients with traumatic brain injury: a systematic review, Int. J. Clin. Exp. Med. 8 (11) (2015) 19881.
[60] R Core Team, R: A Language and Environment for Statistical Computing, R Foundation for Statistical Computing, 2021.
[61] A. Vehtari, A. Gelman, J. Gabry, Practical Bayesian model evaluation using leave-one-out cross-validation and WAIC, Stat. Comput. 27 (5) (2017) 1413–1432.
[62] D.N. Politis, J.P. Romano, M. Wolf, Subsampling, Springer Science & Business Media, 1999.
[63] M.R. Chernick, Bootstrap Methods: A Guide for Practitioners and Researchers, John Wiley & Sons, 2011.
[64] O.B. Bolorunduro, C. Villegas, T.A. Oyetunji, E.R. Haut, K.A. Stevens, D.C. Chang, E. Cornwell III, D.T. Efron, A.H. Haider, Validating the injury severity score (ISS) in different populations: ISS predicts mortality better among Hispanics and females, J. Surg. Res. 166 (1) (2011) 40–44.
[65] E. Jussupow, K. Spohrer, A. Heinzl, J. Gawlitza, Augmenting medical diagnosis decisions? An investigation into physicians' decision-making process with artificial intelligence, Inf. Syst. Res. 32 (3) (2021) 713–735.
[66] Z. Obermeyer, E.J. Emanuel, Predicting the future—big data, machine learning, and clinical medicine, N. Engl. J. Med. 375 (13) (2016) 1216.
[67] D. Ravì, C. Wong, F. Deligianni, M. Berthelot, J. Andreu-Perez, B. Lo, G.-Z. Yang, Deep learning for health informatics, IEEE J. Biomed. Health Inform. 21 (1) (2016) 4–21.
[68] S. Saria, A.K. Rajani, J. Gould, D. Koller, A.A. Penn, Integration of early physiological responses predicts later illness severity in preterm infants, Sci. Transl. Med. 2 (48) (2010).

Gleb Zavadskiy is a fifth-year PhD student at the University of South Florida Muma College of Business. He received his Bachelor's and Master's degree in applied mathematics and physics from Moscow Institute of Physics and Technology in Dolgoprudny, Russia. He is interested in optimization, decision analysis and Bayesian learning.

Daniel Zantedeschi is an Assistant Professor in the School of Information Systems and Management in the Muma College of Business at the University of South Florida. As a trained research methodologist, he creates prescriptive analytics tools at the intersection of Information Systems, Marketing, and Machine Learning. The University of Texas at Austin awarded him a doctorate in Information, Risk, and Operations Management. He also held research and teaching positions at the University of Pennsylvania and the Ohio State University, in addition to the University of South Florida.

Wolfgang Jank holds the Anderson Chair in Global Management. He teaches data mining and statistics to master's, MBA, and Executive MBA students. Jank focuses his research on the application of statistics and data mining to data-driven issues in marketing, IT, and operations management. Jank holds a PhD from UF in statistics and an MA from TU Aachen in mathematics (Germany). Prior to joining the Muma College of Business, he was an associate professor in the Department of Decisions, Operations & Information Technologies, and served as the director of the Center for Complexity in Business at the University of Maryland's Smith School of Business.